ELSEVIER

www.elsevier.nl/locate/jorganchem

Journal of Organometallic Chemistry 612 (2000) 125–132

Journal of Organo metallic Chemistry

Vibrational spectroscopy studies and density functional theory calculations on square-planar vinylidene, carbonyl and ethylene rhodium(I) complexes

D. Moigno [a], W. Kiefer* [a,1], J. Gil-Rubio [b], H. Werner* [b,2]

[a] *Institut für Physikalische Chemie der Universität Würzburg, Am Hubland D-97074 Würzburg, Germany*
[b] *Institut für Anorganische Chemie der Universität Würzburg, Am Hubland D-97074 Würzburg, Germany*

Received 25 January 2000; accepted 15 June 2000

Dedicated to Professor M. Schmidt on the occasion of his 75th birthday.

Abstract

Density functional theory (DFT) calculations have been carried out for *trans*-$[RhF(=C=CH_2)(PMe_3)_2]$ (**5**), *trans*-$[RhF(CO)(PMe_3)_2]$ (**6**) and *trans*-$[RhF(C_2H_4)(PMe_3)_2]$ (**7**) which serve as model compounds for the analysis of the vibrational structure of related rhodium (I) compounds. The calculated structures were in good agreement with the geometries determined from the experimental data of related compounds. The calculated vibrational modes have been used to classify the bands found in the Raman spectra of the rhodium (I) complexes: *trans*-$[RhF(=C=CH_2)(PiPr_3)_2]$ (**1**), *trans*-$[RhF(={}^{13}C={}^{13}CH_2)(PiPr_3)_2]$ (**2**), *trans*-$[RhF(CO)(PiPr_3)_2]$ (**3**) and *trans*-$[RhF(C_2H_4)(PiPr_3)_2]$ (**4**). The comparison of the vibrational behavior of the vinylidene complexes **1** and **2** allow for a characterization of the Rh=C stretching mode. The IR and FT-Raman spectra of complexes **1**–**4** exhibit one vibrational mode between 425 and 465 cm^{-1} with strong to medium intensity. This band can be assigned to the $\nu(RhF)$ mode.

Keywords: Rhodium; Vinylidene complexes; DFT calculations; IR and FT-Raman spectroscopy; Isotopic substitution

---

1. Introduction

Vibrational spectroscopy is one of the most useful tools for obtaining information about the strength of the bonds in a molecule despite the fact that the direct assignment of the infrared or Raman absorptions of relatively complex molecules, as organotransition metal compounds, is rather complicated. Theoretical calculations can certainly assist to obtain a deeper understanding of the vibrational spectra of complicated molecules. In particular, recent developments in DFT [1] have shown that DFT is a powerful computational alternative to the conventional quantum chemical methods, since they are much less computationally demanding and take account of the effects of electron correlation. In addition, the use of atomic effective core potentials (ECP) and model potentials (MP) [2] to eliminate chemically inactive atomic core electrons from quantum chemical calculations has gained widespread acceptance, also in calculations of transition metal complexes [3]. The methods based on DFT are known to offer promise of obtaining accurate vibrational wavenumbers [4] and, in fact, have been used in the study of vibrational spectra of a variety of molecular systems including organotransition metal complexes [5]. One of the most relevant features of the vibrational spectra of this class of compounds are the metal–carbon stretching vibrations, since they are directly related to such a substantial property of the molecule as the M–C bond strength. However, the assignment of the $\nu(MC)$ vibrational modes is very often quite complicated due to the presence of other bands in the same region or of their low intensity. By using isotopic substitution, in conjunction with theoretical calculations, it has been possi-

---

[1] *Corresponding author. Tel.: +49-931-8886330; fax: +49-931-8886332; e-mail: wolfgang.kiefer@mail.uni-wuerzburg.de

[2] *Corresponding author. Fax: +49-931-888-4605; e-mail: helmut.werner@mail.uni-wuerzburg.de

PII: S0022-328X(00)00430-7

ble to bypass these difficulties and to do an exact assignment.

In order to gain more information about the properties of the metal–carbon multiple bond, we have been interested in the determination of the metal–carbon stretching vibrational mode in vinylidene complexes. While many vibrational studies are available for carbonyl complexes [5–7], very few studies have been carried out in transition-metal carbene or carbyne complexes [7,8]. In this paper we report the first vibrational spectroscopic study on vinylidene complexes. This study has been carried out on the compounds *trans*-[RhF(=C=CH$_2$)(P*i*Pr$_3$)$_2$] (**1**) and *trans*-[RhF(=^{13}C=^{13}CH$_2$)(P*i*Pr$_3$)$_2$] (**2**), whose IR and FT-Raman spectra have been measured and assigned with the help of DFT calculations using the model compounds *trans*-[RhF(=C=CH$_2$)(PMe$_3$)$_2$] (**5**), *trans*-[RhF(CO)(PMe$_3$)$_2$] (**6**) and *trans*-[RhF(C$_2$H$_4$)(PMe$_3$)$_2$] (**7**). The vibrational spectra of the compounds *trans*-[RhF(CO)(P*i*Pr$_3$)$_2$] (**3**) and *trans*-[RhF(C$_2$H$_4$)(P*i*Pr$_3$)$_2$] (**4**) have been also measured, assigned and compared with those of **1** and **2**.

Table 1
Selected bond lengths (pm) and angles (°) calculated for the model compound **5** together with the experimental values found in *trans*-[RhCl(C=CHMe)(P*i*Pr$_3$)$_2$]

	trans-[RhF(C=CH$_2$)(PMe$_3$)$_2$ (**5**)			*trans*-[RhCl(C=CHMe)(P*i*Pr$_3$)$_2$]
	Calc. [a]	Calc. [b]	Calc. [c]	Exp. [d]
Bond lengths				
Rh–P$_1$	238.5	234.4	229.3	234.4(2)
Rh–P$_2$	238.5	234.4	229.3	234.2(2)
Rh–X	205.5	206.1	199.8	236.6(2)
Rh–C$_1$	182.0	181.0	178.2	177.5(6)
C$_1$–C$_2$	134.1	133.3	132.7	132.0(1)
Bond angles				
P$_1$–Rh–P$_2$	169.2	170.3	177.6	173.9(1)
X–Rh–C$_1$	179.4	180.0	180.0	175.8(2)
P$_1$–Rh–X	84.6	85.2	88.8	91.9(1)
P$_1$–Rh–C$_1$	95.4	94.8	91.2	88.2(2)
P$_2$–Rh–X	84.6	85.2	88.8	91.2(1)
P$_2$–Rh–C$_1$	95.4	94.8	91.2	89.1(2)
Rh–C$_1$–C$_2$	179.6	179.4	180.0	177.9(6)

[a] Calculated with BPW91/LANL2DZ.
[b] Calculated with BPW91/LANL2DZ+(d).
[c] Calculated with BPW91/ECPII.
[d] Ref. [11].

Table 2
Selected bond lengths (pm) and angles (°) calculated for the model compound **6** together with the experimental values found in *trans*-[RhF(CO)(PPh$_3$)$_2$]

	trans-[RhF(CO)(PMe$_3$)$_2$] (**6**)			*trans*-[RhF(CO) (PPh$_3$)$_2$]
	Calc. [a]	Calc. [b]	Calc. [c]	Exp. [d]
Bond lengths				
Rh–P$_1$	238.5	234.1	231.7	233.0(7)
Rh–P$_2$	238.5	234.1	231.7	232.4(7)
Rh–X	205.2	205.8	197.7	204.6(2)
Rh–C$_1$	181.8	181.6	176.2	179.6(3)
C–O	120.9	118.3	118.6	115.1(4)
Bond angles				
P$_1$–Rh–P$_2$	165.3	167.0	175.6	174.3(3)
X–Rh–C$_1$	179.8	179.7	180.0	
P$_1$–Rh–X	82.7	83.5	87.8	86.9(5)
P$_1$–Rh–C$_1$	97.3	96.5	92.2	91.3(5)
P$_2$–Rh–X	82.7	83.5	87.8	88.1(9)
P$_2$–Rh–C$_1$	97.3	96.5	92.2	93.7(9)

[a] Calculated with BPW91/LANL2DZ.
[b] Calculated with BPW91/LANL2DZ+(d).
[c] Calculated with BPW91/ECPII.
[d] Ref. [9].

Table 3
Selected bond lengths (pm) and angles (°) of complexes **7** (calculated) and **4** (experimental)

	trans-[RhF(C$_2$H$_4$)(PMe$_3$)$_2$] (**7**)			*trans*-[RhF(C$_2$H$_4$)(P*i*Pr$_3$)$_2$] (**4**)
	Calc. [a]	Calc. [b]	Calc. [c]	Exp. [d]
Bond lengths				
Rh–P$_1$	237.4	233.3	231.6	232.6(2)
Rh–P$_2$	237.4	233.3	231.6	232.8(2)
Rh–F	206.7	207.2	197.5	206.0(3)
Rh–C$_1$	213.9	212.1	209.7	209.6(5)
Rh–C$_2$	214.6	212.4	210.6	210.3(5)
C$_1$–C$_2$	144.2	143.1	143.9	138.0(8)
Bond angles				
P$_1$–Rh–P$_2$	164.8	165.8	171.8	169.5(5)
F–Rh–C$_1$	160.0	159.5	158.9	160.4(2)
F–Rh–C$_2$	160.6	161.1	161.0	161.2(2)
P$_1$–Rh–F	82.4	82.9	85.9	85.7(9)
P$_2$–Rh–F	82.4	82.9	85.9	84.7(9)
P$_1$–Rh–C$_1$	97.1	96.7	93.8	93.8(2)
P$_2$–Rh–C$_1$	97.1	96.7	93.8	93.8(2)
P$_1$–Rh–C$_2$	97.2	96.7	93.8	95.6(2)
P$_2$–Rh–C$_2$	97.2	96.7	93.8	94.8(2)
C$_1$–Rh–C$_2$	39.4	39.4	40	38.4(2)

[a] Calculated with BPW91/LANL2DZ.
[b] Calculated with BPW91/LANL2DZ+(d).
[c] Calculated with BPW91/ECPII.
[d] Ref. [10].

2. Results and discussion

2.1. DFT calculations

The structural parameters of the model compounds *trans*-[RhF(=C=CH$_2$)(PMe$_3$)$_2$] (**5**), *trans*-[RhF(CO)(PMe$_3$)$_2$] (**6**) and *trans*-[RhF(C$_2$H$_4$)(PMe$_3$)$_2$] (**7**), which were calculated using the BPW91/LANL2DZ, BPW91/LANL2DZ+(d) and BPW91/ECPII methods, are summarized in Tables 1–3. One may notice that the computed structures are distorted square-planar with the phosphines in an eclipsed conformation (Fig. 1). The methods described above, were applied to a molecular geometry without symmetry restrictions and to a geometry that was restricted to C_{2v} symmetry. Analytical harmonic vibrational modes have also been calculated for all the structures to confirm that a local minimum on the potential energy surface was found. Using the C_{2v} symmetry, the rotational conformations of the phosphine groups (estimated barrier of rotation < 2.09 kJ mol^{-1}) caused difficulties with convergence and the optimization yielded structures with two low imaginary harmonic wavenumbers corresponding to the M–PR_3 rotations which indicated a saddle point. After many attempts to circumvent this problem the calculations were carried out using a C_1 symmetry. One may notice that the calculated geometry with C_1 symmetry is very close to the one expected for the C_{2v} symmetry. It should be noted further, that the C_{2v} symmetry of the rhodium complexes in crystalline state is broken.

The calculated Rh–F and Rh–P bond distances are similar to the experimental values found in the related fluororhodium complexes *trans*-[RhF(CO)$(PPh_3)_2$] [9] and *trans*-[RhF(C_2H_4)(P*i*$Pr_3)_2$] (**4**) [10] and in *trans*-[RhCl(=C=CHMe)(P*i*$Pr_3)_2$] [11]. In the model compounds **5–7**, the phosphine ligands are slightly bent toward the fluorine atom probably owing to the electrostatic attraction between the negatively charged fluoride and the positively charged phosphorus atoms. A similar bending has been observed in the crystal structures of **4** and *trans*-[RhF(CO)$(PPh_3)_2$].

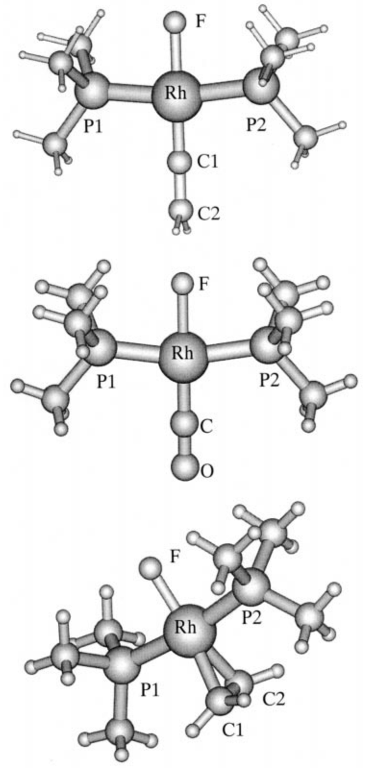

Fig. 1. Optimized structures of *trans*-[RhF(=C=CH_2)$(PMe_3)_2$] (**5**), *trans*-[RhF(CO)$(PMe_3)_2$] (**6**) and *trans*-[RhF$(C_2H_4)(PMe_3)_2$] (**7**) using the BPW91/LANL2DZ method.

As expected, the Rh–C_1–C_2 linkage of **5** is almost linear and the plane which contains the vinylidene ligand is perpendicular to the main plane containing the atoms Rh, P_1, P_2 and F (the dihedral angle between the main planes defined by the atoms [Rh, C_1, C_2, H_1, H_2] and [Rh, P_1, P_2, F] is 90.0°). This structural feature is in agreement with the formation of a π bond between Rh and C_1 and confirms the formal analogy between allenes and vinylidene metal complexes. The computed Rh–C_1 distances of the model compounds **5** and **6** are comparable with the Rh–C bond lengths in the fluoro carbonyl rhodium (I) compound *trans*-[RhF(CO)$(PPh_3)_2$] (179.6(3) pm) [9] and in *trans*-[RhCl(=C=CHMe)(P*i*$Pr_3)_2$] (177.5(6) pm) [11]. For the complexes **5–7**, the Rh–F distances were better reproduced by the BPW91/LANL2DZ and LANL2DZ + (d) methods, with values around 205 pm, which are very close to the experimental data found in *trans*-[RhF(CO)$(PPh_3)_2$] (204.6(2) pm) and **4** (206.0(3) pm). In contrast, the Rh–C and Rh–P distances were closer to the experimental values when the BPW91/ECPII or BPW91/LANL2DZ + (d) methods were used.

It is remarkable that the BPW91/LANL2DZ method shows a high accuracy for the Rh–F bond lengths which is certainly fortuitous but one must note that this method fails in the calculation of the Rh–X (X = Cl, Br and I) bond lengths [15]. This can be attributed to the fact that the basis set, which is used in these calculations, is too small for a complete description of the system. The additional use of diffuse and polarization function (Tables 1–3) is more reliable in the determination of the structures.

2.2. Vibrational spectroscopy

In order to identify in the Raman spectra of the rhodium complexes the characteristic vibrational modes of P*i*Pr_3 ligands, a Raman spectrum of the liquid ligand was measured and assigned. Extensive vibrational spectroscopic investigations of isopropylhalides reported by Klaboe [12] have been used as a tool to assign most of the vibrational modes of the *i*Pr groups.

The P-C vibrational modes have been identified and assigned by comparison with the assignment made by Holmes and co-workers [13]. The ν(CH) vibrations of P*i*Pr_3 have been located between 2850 and 3000 cm^{-1}; the $\delta(CH_3)$ modes lie in the spectral range between 1350 and 1480 cm^{-1} and the rocking modes between 900 and 1160 cm^{-1}. Fig. 2 presents the low wavenumber region of the Raman spectrum of triisopropylphos-

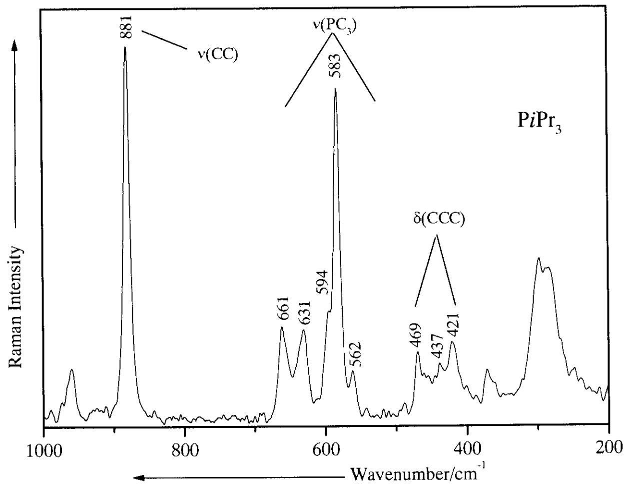

Fig. 2. The low-wavenumber region of the FT-Raman spectrum of P*i*Pr$_3$.

phine. The strong band at 881 cm^{-1} corresponds to the ν(CC) vibration. The characteristic ν(PC$_3$) modes are observed in the 500–700 cm^{-1} spectral region, the asymmetric one at higher wavenumbers and the symmetric one as a strongly polarized Raman band around 560 cm^{-1}. The (CC$_3$)–, (CPC)– and (PCC)– deformation modes are present between 200 and 500 cm^{-1} in the Raman spectrum of **1**–**4**. The δ_s(CCC) mode appeared around 420 cm^{-1}.

For the assignment of the vibrations of the F–Rh=C=CH$_2$ skeleton of complex **1** and its ^{13}C-analogue **2**, DFT-calculations carried out on the model compound *trans*-[RhF(=C=CH$_2$)(PMe$_3$)$_2$] (**5**) have been used. The calculated and experimental wavenumbers are displayed in Table 4.

The ν(C=C) vibration is only IR active for complexes **1** and **2**, giving two close bands which are significantly shifted by ca. 46 cm^{-1} to lower wavenumbers in the ^{13}C-containing compound **2** (Fig. 3). The in plane δ(CH$_2$) mode was found at 1326 cm^{-1} in the IR spectrum of **1**, which, as expected, is shifted to lower wavenumbers in **2**. In the IR spectrum of **2**, the new band at 1518 cm^{-1} was temptatively assigned to an overtone of the ν(CH$_2$) wagging mode at 759 cm^{-1} (Fig. 4). The latter band is shifted by 7 cm^{-1} to lower wavenumbers compared to **1**.

According to the DFT calculation, the ν(RhC) mode should appear around 571 cm^{-1}. The assignment of the bands at 574 cm^{-1} and 572 cm^{-1} in the IR (Fig. 4) and Raman spectrum (Fig. 5) of complex **1**, respectively, was rather complicated due to the presence of the ligand P*i*Pr$_3$ bands in the same region. Comparing the Raman spectra of **1** and **2** (Fig. 5), the band at 572 cm^{-1} could be exactly assigned to the ν(RhC) mode, since this band was shifted to 559 cm^{-1} for the ^{13}C-containing complex **2**. In addition, the wavenumbers corresponding to the ν(^{13}C=^{13}C), ν(Rh^{13}C) and ν(RhF) stretching modes were calculated with the BPW91/LANL2DZ method. The resulting values (1594, 556 and 450 cm^{-1}, respectively) are also in good agreement with the experimental data ($\Delta\nu_{(\mathrm{RhC})\mathrm{calc.}} = 15$ cm^{-1} vs. $\Delta\nu_{(\mathrm{RhC})\mathrm{exp.}} = 13$ cm^{-1} and $\Delta\nu_{(\mathrm{C=C})\mathrm{calc.}} = 62$ cm^{-1} vs. $\Delta\nu_{(\mathrm{C=C})\mathrm{exp.}} = 46$ cm^{-1}). The larger difference for the last value can probably be attributed to the higher anharmonicity of this mode. Thus, the weak band at 577 cm^{-1} in the Raman spectra of **2** was assigned to the ν(PC$_3$) vibration. In the IR spectrum of **2** (Fig. 4), two bands of medium and weak relative intensity were observed at 574 cm^{-1} and 559 cm^{-1}, respectively. We interpreted this result by postulating that, in contrast with the Raman spectra, in the IR spectra of **1** and **2** the ν(PC$_3$) bands are more intense than the ν(RhC) bands. Thus, the IR band at 574 cm^{-1} corresponds to the ν(PC$_3$) mode of the phosphine, and should have the same wavenumber for **1** and **2**. In the IR spectrum of **1**, the ν(RhC) band could be hidden by the ν(PC$_3$) band, but it is observed at 559 cm^{-1} in the IR spectrum of **2**. The ν(RhF) band of **1** was assigned to the strong IR and medium Raman band at 458 cm^{-1}. Visual inspection of the animated vibrational modes showed clearly that the Rh–C and Rh–F stretching vibrations are weakly coupled. This coupling could be responsible for the observed shift by 4 cm^{-1} of the Rh–F stretching band in compound **2**.

For complexes of the type *cis*[MX$_2$(CO)$_2$]$^-$ (X = Cl, Br) (M = Rh, Ir), Browning et al. [14] assigned the ν(MC) stretching mode to the strongest Raman band and the δ(MCO) to the strongest IR bands in the 400–700 cm^{-1} region. In the related compounds *trans*-[RhX(CO)(PMe$_3$)$_2$] (X = Cl, Br), the same authors assigned the ν(RhC) stretching mode at 550 and 552 cm^{-1} and the ν(CO) stretching mode at 1965 and 1961 cm^{-1} for the chloride and bromide substituted complexes, respectively. The FT-Raman spectrum of the carbonyl compound **3** exhibited a strong band at 1929 cm^{-1}, which was assigned to the ν(CO) vibration (Fig. 6). The assignments of the ν(RhC) and ν(RhF) vibrational modes at 573 and 465 cm^{-1}, respectively (Table 3), are in good agreement with the calculated ν(RhC) and ν(RhF) stretching wavenumbers of the model complex **6** (571 and 451 cm^{-1}). The calculations showed that both ν(RhC) and ν(RhF) vibrational modes are weakly coupled as in the vinylidene derivatives. The ν(PC$_3$) band could also overlap with the ν(RhC) band on the analogy of **1**.

The coincidence in wavenumber of the Rh–C stretching mode for compounds **1** and **3**, which contain the isoelectronic ligands C=CH$_2$ and CO suggests a stronger Rh–C bond strength in the carbonyl complex. Since the complexes **2** and **3** possess the same reduced mass (^{13}C=^{13}CH$_2$ vs. CO), a comparison of the FT-Raman spectra allow for an evaluation of the bonding strength free of any mass effects and therefore only showing effects of electronic nature. Thus, a direct comparison of the ν(RhC) stretching modes of complex **2** (559 cm^{-1}) and **3** (573 cm^{-1}) allows to point out the difference in the RhC bond strength of the mentioned complexes. Furthermore, the ν(RhF) stretching mode is also 11 cm^{-1} blue shifted in complex **3**. From this, one can see that the carbonyl ligand is a better π-acceptor and a less effective σ-donor than the vinylidene one.

Comparing the values of ν(CO) and ν(RhC) for compound **3** with the values found in *trans*-[RhX(CO)(PMe$_3$)$_2$] [13a] (for X = Cl and Br, ν(CO) = 1965 and 1961 cm^{-1}, ν(RhC) = 550 and 552 cm^{-1}, respectively) or *trans*-[RhCl(CO)(P*i*Pr$_3$)$_2$] (ν(CO) = 1938 cm^{-1}, ν(RhC) = 559 cm^{-1}) [15] one may notice that the Rh–C bond is stronger in **3**. This difference can be attributed to the higher Lewis basicity of P*i*Pr$_3$ and to the effect of the fluoro ligand which, in spite of its higher electronegativity, acts as a better π donor than Cl and Br [16]. The band at 601 cm^{-1} of high relative intensity in the IR spectrum of **3**, shows a 19 cm^{-1} red shift in the *trans*-[RhCl(CO)(P*i*Pr$_3$)$_2$] complex due to the different Rh–C bond strength of the fluoro and chloro complex. The weak band at 558 cm^{-1} and the band at 601 cm^{-1} in the IR spectrum, which did not appear in the spectra of **1** and **4**, can be attributed to the δ(RhCO) modes. For the *trans*-[RhCl(CO)(P*i*Pr$_3$)$_2$] complex, there was a photodecomposition under the laser excitation, which did not allow the recording of a Raman spectrum. The influence of the *trans* halogen ligand on the M–C bond strength reflects the shift of the vibrational bending mode.

The bonding in alkene complexes can be described by two models, the synergistic ligand → metal σ-donation and ligand ← metal π-back-donation of Dewar [17] and, Chatt and Duncanson [18], and the model where there are two electronsharing metal–carbon σ-bonds,

Table 4
Selected calculated and experimental fundamental vibrational wavenumbers (cm^{-1}) for *trans*-[RhFL(PR$_3$)$_2$] complexes together with their tentative assignment

1 Exp.		5 Calc.	2 Exp.		3 Exp.		6 Calc.	4 Exp.		7 Calc.	Assignment
R	IR		R	IR	R	IR		R	IR		
					1929s	1934vs	1843 ^{a} 1952 ^{b}				ν(CO)
	1628s	1656 ^{a} 1654 ^{b} 1594 ^{c}		1582							ν(C=C)
								1506vw	1506m	1495 ^{a} 1501 ^{b}	ν(C=C) + δ(CH$_2$)
	1326 w	1340 ^{a} 1311 ^{b}		1318							δ(CH$_2$)
								1197s	1197s	1188 ^{a} 1187 ^{b}	ν(C=C) + δ(CH$_2$)
								1183vw	1183w	1180 ^{a} 1168 ^{b}	Twist τ(CH$_2$) ethylene
884vs	884s		885vs	885s	885vs	885s		885vs	882s		ν(CC)
									801m	791 ^{a} 782 ^{b}	Rocking ρ(CH$_2$) ethylene
					601vw	601s	563 ^{a} 567 ^{b}				δ(RhCO)
					558shw	542m	511 ^{a} 513 ^{b}				
572vs	572m	571 ^{a} 570 ^{b} 556 ^{c}	559vs	559m	573vs	573m	571 ^{a} 561 ^{b}				ν(Rh=C)
								514mw	514mw	470 ^{a} 477 ^{b}	ν(RhC)$_{asym}$
458m	458vs	451 ^{a} 433 ^{b} 450 ^{c}	454m	454vs	465m	465s	450 ^{a} 434 ^{b}			456 ^{a}	ν(RhF)
								471m	471m	448 ^{b}	ν(RhF) + ν(RhC)$_{sym}$
								425vs	425vs	409 ^{a} 404 ^{b}	ν(RhF)
340w		323 ^{a} 328 ^{b}	341w		341w		330 ^{a} 331 ^{b}	349w		321 ^{a} 330 ^{b}	ν(RhP)$_{sym}$
308m		317 ^{a} 313 ^{b}	307m		305m		320 ^{a} 321 ^{b}	306m		320 ^{a} 311 ^{b}	ν(RhP)$_{asym}$

[a] Calculated with BPW91/LANL2DZ.
[b] Calculated with BPW91/LANL2DZ+(d).
[c] Calculated for the isotopic vinylidene with BPW91/LANL2DZ. Abbreviations: s, m, w = strong, medium, weak, respectively; v = very.

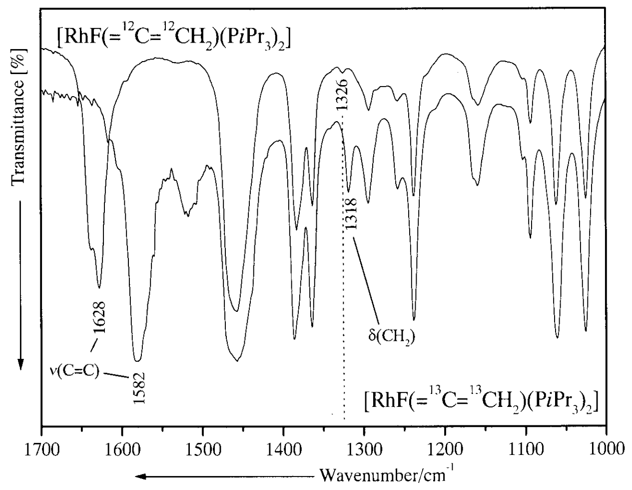

Fig. 3. The high-wavenumber region of the IR spectra of *trans*-[RhF(=C=CH$_2$)(P*i*Pr$_3$)$_2$] (**1**) and *trans*-[RhF(=^{13}C=^{13}CH$_2$)(P*i*Pr$_3$)$_2$] (**2**).

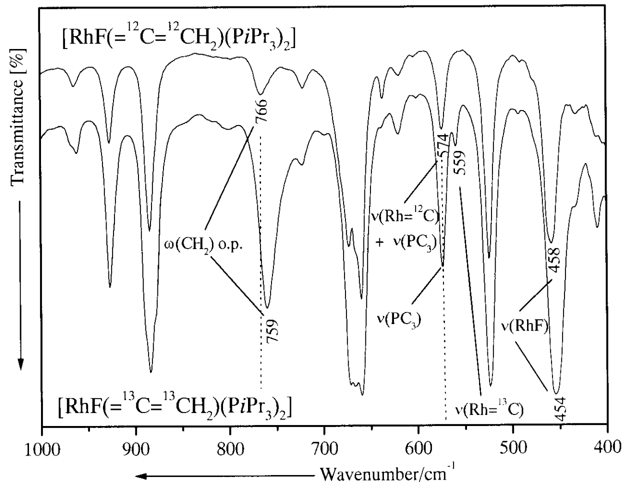

Fig. 4. The low-wavenumber region of the IR spectra of *trans*-[RhF(=C=CH$_2$)(P*i*Pr$_3$)$_2$] (**1**) and *trans*-[RhF(=^{13}C=^{13}CH$_2$)(P*i*Pr$_3$)$_2$] (**2**).

forming a metallacyclopropane ring. In molecules described by the first model, only one metal–carbon stretching band is expected, while in metallacyclopropane-type compounds two bands, one symmetrical and one unsymmetrical, are expected [6,19,20]. In our case, the calculations carried out for the model compound **7** suggested that compound **4** is best described by the second model, since two ν(RhC) modes were obtained, both weakly coupled with the ν(RhF) vibration. The calculated wavenumbers were 514 (asymmetric) and 471 (symmetric) cm^{-1}.

A vibration which is mainly Rh–F stretching in character was calculated at 409 cm^{-1}. The band observed in the IR and Raman spectra of **4** at 514 cm^{-1} (Fig. 7) was tentatively assigned to the asymmetric Rh–C stretching mode. The intense and medium bands at 425 and 471 cm^{-1}, respectively, could be due to the Rh–F and the asymmetric Rh–C stretching modes. Some bands are observed as for the vinylidene and carbonyl complexes in the IR and Raman spectrum between 534 and 432 cm^{-1}. These bands could be assigned to (CC$_3$)–, (CPC)– deformation modes.

The ν(C=C) vibrational mode for complex **5** was observed at 1506 cm^{-1} in the IR- and FT-Raman spectrum (Fig. 7). This value is close to the calculated one (1495 cm^{-1}) for the model compound **7**. The ν(C=C) wavenumber is 117 cm^{-1} lower than that of gaseous ethylene (1623 cm^{-1}) [21] and also slightly lower than that of ν(C=C) band of [RhCl(C$_2$H$_4$)(P*i*Pr$_3$)$_2$] (1510 cm^{-1}) [22]. This result is in agreement with the observed C=C bond distances: 131.9(4) pm for the chloro complex [22] and 138.0(8) pm for the fluoro analogue [10]. Nevertheless, only the decrease in the ν(C=C) wavenumber alone can not be used as a measure of the M–C$_2$H$_4$ bond strength, since

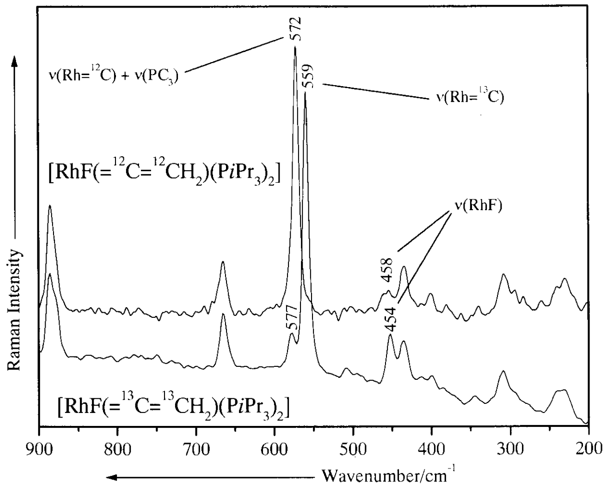

Fig. 5. The low-wavenumber region of the FT-Raman spectra of *trans*-[RhF(=C=CH$_2$)(P*i*Pr$_3$)$_2$] (**1**) and *trans*-[RhF(=^{13}C=^{13}CH$_2$)(P*i*Pr$_3$)$_2$] (**2**).

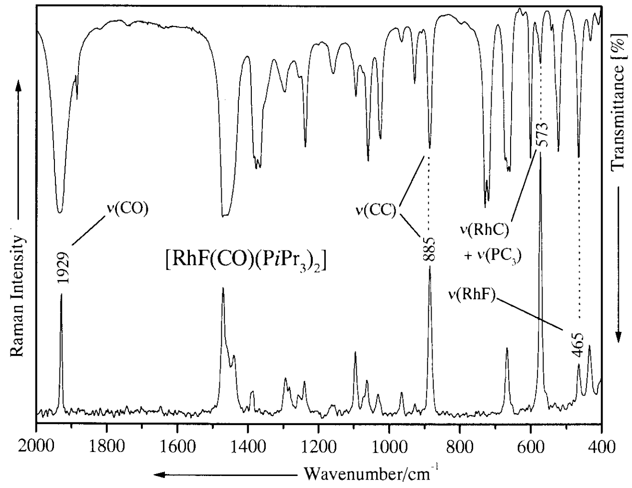

Fig. 6. The IR and FT-Raman spectra of *trans*-[RhF(CO)(P*i*Pr$_3$)$_2$] (**3**).

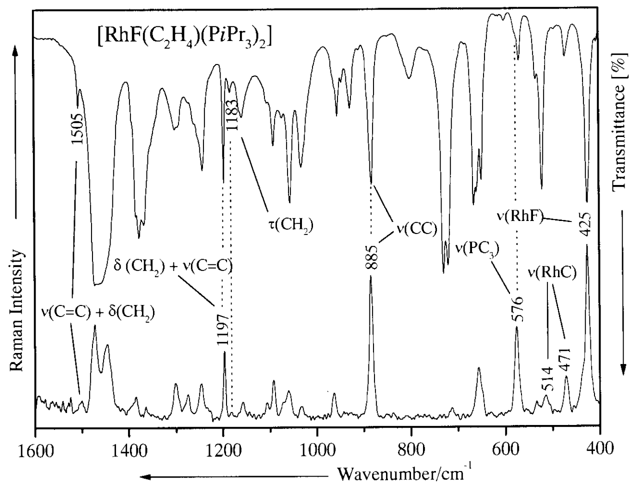

Fig. 7. The IR and FT-Raman spectra of *trans*-$[RhF(C_2H_4)(P{\it i}Pr_3)_2]$ (**4**).

the calculations carried out on $[PtCl_3(C_2H_4)]^-$ [19], $[PdCl_3(C_2H_4)]^-$ [20] and on our model complex **7** show that the C=C stretching vibration is strongly coupled with the in-plane CH_2 scissoring mode. The band at 1197 cm^{-1}, which did not appear in the FT-Raman spectrum of **1**, was attributed to the $\delta(CH_2)$ mode of the ethylene ligand. This band was calculated at 1188 cm^{-1} and is also strongly coupled with the ν(C=C) mode.

3. Conclusions

The metal–carbon stretching modes in complexes containing metal–carbon multiple bonds are extremely useful data but its assignment is often very complicated. In this study, we have used DFT calculations to assign the IR and Raman band positions for the square-planar rhodium(I) complexes *trans*-$[RhFL(P{\it i}Pr_3)_2]$, with L = $C{=}CH_2$ (**1**), CO (**3**) and $H_2C{=}CH_2$ (**4**). These calculations have been carried out using the model compounds *trans*-$[RhFL(PMe_3)_2]$ (**5**–**7**). The assignment of the ν (Rh=C) bands in the vinylidene complex **1** has been confirmed by isotopic substitution and allows us to study the influence of the *trans* disposed ligand on Rh=C bond by means of FT-Raman spectroscopy. A comparison between the ν (RhC) wavenumbers of compounds **2** and **3**, containing the isoelectronic ligands $^{13}C{=}^{13}CH_2$ and CO, which have the same reduced mass, indicated that the Rh–C bond is stronger in the carbonyl than in the vinylidene complex. The calculated vibrational modes support the description of the ethylene complex **4** as a metallacyclopropane. The IR and FT-Raman spectra of complexes **1**–**4** exhibit one band between 437 and 465 cm^{-1} of medium to weak relative intensity which was assigned to the ν (RhF) mode.

4. Experimental

Compounds **1** [23], **3** and **4** [10] were prepared by using reported procedures. Compound **2** was prepared analogously to **1** but using $^{13}C_2H_2$ (Cambridge Isotope Laboratory) instead of $^{12}C_2H_2$. NMR data of **2**: ^1H-NMR (C_6D_6, 200 MHz) δ 2.59 (m, 6H, $PCHCH_3$), 1.33 (d of virtual t, $^3J(HH) = 6.5$ Hz, N = 13.6 Hz, 36H, $PCHCH_3$), 0.05 (br d, $^1J(CH) = 161.0$ Hz, 2H, $^{13}CH_2$); ^{13}C NMR (C_6D_6, 50.3 MHz) δ 297.1 (dddt, $J(RhC) =$ 51.1 Hz, $J(PC) = 16.1$ Hz, $J(FC) = 92.7$ Hz, $J(CC) =$ 56.8 Hz, Rh=C), 88.4 (br d, $J(CC) = 56.8$ Hz, CH_2), 22.9 (virtual t, N = 18.5 Hz, $PCHCH_3$), 20.0 (s, $PCHCH_3$); ^{19}F-NMR (C_6D_6, 188.3 MHz) δ − 222.4 (br d, $J(FC) = 92.7$ Hz); ^{31}P-NMR (C_6D_6, 81 MHz) δ 45.4 (br d, $J(RhP) = 145.0$ Hz, $^3J(PC) = 4.8$ Hz).

The NMR spectra were measured at room temperature using a Bruker AC 200 instrument. The FT-Raman spectra were recorded at room temperature using a Bruker IFS 120-HR spectrometer with an adapted FRA 106 Raman module (resolution = 3 cm^{-1}). Radiation of 1064 nm from a Nd-YAG laser was employed for excitation of solid samples contained in NMR tubes. The infrared spectra were recorded with a Bruker IFS 25 spectrometer using nujol suspensions between KBr plates.

4.1. Computational details

The DFT calculations were performed using Gaussian 98 [24] and Becke's 1988 exchange functional [25] in combination with the Perdew–Wang 91 gradient-corrected correlation functional (BPW91) [26]. The Los Alamos effective core potential plus double zeta (LANL2DZ) [27–29] was employed for rhodium, whereas the Dunning/Huzinaga full double zeta basis set with or without polarization and diffuse function (D95 or D95 + (d)) was used for the other atoms (all first row-element). The following contraction patterns [30] (441/2111/41) with the Hay–Wadt ECP-Rh 3-28 for rhodium [29,31] and the 6-31 + G(d) Pople basis set for the other atoms. The last method is denoted ECPII in this paper.

Acknowledgements

Financial support from the Deutsche Forschungsgemeinschaft (Sonderforschungsbereich SFB 347) and the European Commission (Contract ERBFMBICT960698) as well as from the Fonds der Chemischen Industrie is gratefully acknowledged. We are also grateful to the Degussa AG for various gifts of chemicals.

References

[1] (a) R.G. Parr, W. Yang, Density Functional Theory of Atoms and Molecules, Oxford University Press, Oxford, 1989. (b) J.M. Seminario, P. Politzer, Modern Density Functional Theory, a Tool for Chemistry, Elsevier Science B.V., Amsterdam, The Netherlands, 1995.

[2] (a) J.C. Berthelat, P.P. Durand, Gazz. Chim. Ital. 108 (1978) 225. (a) K. Krauss, W. Stevens, J. Annu. Rev. Phys. Chem. 35 (1984) 357. (c) P.A. Christiansen, W.C. Ermler, K.S. Pitzer, Annu. Rev. Phys. Chem. 36 (1985) 407. (d) L. Szas, Pseudopotential Theory of Atoms and Molecules, Wiley, New York, 1983. (e) K. Balasubramanian, K.S. Pitzer, Adv. Chem. Phys. 67 (1987) 287. (f) P. Durand, J.P. Maalrieu, Adv. Chem. Phys. 67 (1987) 321.

[3] G. Frenking, I. Antes, M. Böhme, S. Dapprich, A.W. Ehlers, V. Jonas, A. Neuhaus, M. Otto, R. Stegmann, A. Veldkamp, S.F. Vyboishchikov, in: K.B. Lipkowitz, D.B. Boyd (Eds.), Reviews in Computational Chemistry, vol. 8, VCH, New York, 1996.

[4] B.G. Johnson, P.M.W. Gill, J.A. Pople, J. Chem. Phys. 98 (1993) 5612.

[5] (a) A. Berces, T. Ziegler, J. Phys. Chem. 98 (1994) 13233. (b) A. Berces, T. Ziegler, J. Chem. Phys. 98 (1993) 4793. (c) V. Jonas, W. Thiel, J. Chem. Phys. 102 (1995) 8474. (d) V. Jonas, W.Thiel, J. Chem. Phys. 105 (1996) 3636.

[6] K. Nakamoto, Infrared and Raman Spectra of Inorganic and Coordination Compounds, Wiley, New York, 1986.

[7] G. Frenking, N. Fröhlich, Chem. Rev. 100 (2000) 717.

[8] (a) S.-C. Chang, R.H. Hauge, Z.H. Kafafi, J.L. Margrave, W.E. Billups, J. Am. Chem. Soc. 110 (1988) 7975. (b) E. Diana, O. Gambino, R. Rossetti, P.L. Stanghellini, T. Albiez, W. Bernhardt, H. Vahrenkamp, Spectrochim. Acta 49A (1993) 1247. (c) C.E. Anson, N. Sheppard, D.B. Powell, J.R. Norton, W. Fischer, R.L. Keiter, B.F.G. Johnson, J. Lewis, A.K. Bhattacharrya, S.A.R. Knox, M.L. Turner, J. Am. Chem. Soc. 116 (1994) 3058. (d) E.O. Fischer, N.Q. Dao, W.R. Wagner, Angew. Chem. 90 (1978) 51; Angew. Chem. Int. Ed. Engl. 17 (1978) 50. (e) G.R. Clark, K. Marsden, W.R. Roper, L.J. Wright, J. Am. Chem. Soc. 102 (1980) 6570. (f) N.Q. Dao, E.O. Fischer, T.L. Lindner, J. Organomet. Chem. 209 (1981) 323. (g) N.Q. Dao, H. Fevrier, M. Jouan, E.O. Fischer, W. Röll, J. Organomet. Chem. 275 (1984) 191. (h) J.K. Manna, R.J. Kuk, R.F. Dallinger, M.D. Hopkins, J. Am. Chem. Soc. 116 (1994) 9793. (i) M. Barnes, D.A. Gillet, A.J. Merer, G.F. Metha, J. Chem. Phys. 105 (1996) 6168. (j) R.M. Sosa, P. Gardiol, G. Beltrame, Int. J. Quantum. Chem. 69 (1998) 371.

[9] A. Wierzbicki, E.A. Salter, N.W. Hoffman, E.D. Stevens, L. Van Do, M.S. VanLoock, F.D. Madura, J. Phys. Chem. 100 (1996) 11250.

[10] J. Gil-Rubio, B. Weberndörfer, H. Werner, J. Chem. Soc. Dalton Trans. (1999) 1437.

[11] H. Werner, F.J. Garcia Alonso, H. Otto, J. Wolf, Z. Naturforsch. B 43 (1988) 722.

[12] P. Klaboe, Spectrochim. Acta 26A (1970) 87.

[13] R.R. Holmes, G.T. Fey, R.H. Larkin, Spectrochim. Acta 29A (1973) 665.

[14] J. Browning, P.L. Goggin, R.J. Goodfellow, M.G. Norton, J.M.A. Rattray, B.F. Taylor, J. Mink, J. Chem. Soc. Dalton (1977) 2061.

[15] D. Moigno, J. Gil-Rubio, B. Callejas Gaspar, H. Werner, W. Kiefer, unpublished results.

[16] N.M. Doherty, N.W. Hoffman, Chem. Rev. 91 (1991) 553.

[17] M.J.S. Dewar, Bull. Soc. Chim. Fr. 18 (1951) C79.

[18] J. Chatt, L.A. Duncanson, J. Chem. Soc. (1953) 2929.

[19] M.J. Grogan, K. Nakamoto, J. Am. Chem. Soc. 88 (1966) 5454.

[20] É. Bencze, I. Pápai, J. Mink, P.L. Goggin, J. Organomet. Chem. 584 (1999) 118.

[21] J. Weidlein, U. Müller, K. Dehnicke, Schwingungsspektroskopie, 2. Auflage, Georg Thieme, Stuttgart, New York, 1988.

[22] C. Bussetto, A. D'Alfonso, F. Maspero, G. Perego, A. Zazzetta, J. Chem. Soc. Dalton Trans. (1977) 1828.

[23] J. Gil-Rubio, M. Laubender, H. Werner, Organometallics 19 (2000) 1365.

[24] Gaussian 98, Revision A7, M.J. Frisch, G.W. Trucks, H.B. Schlegel, P.M.W. Gill, B.G. Johnson, M.A. Robb, J.R. Cheeseman, T. Keith, G.A. Petersson, J.A. Montgomery, K. Rhaghavachari, M.A. Al-Laham, V.G. Zakrzewski, J.V. Ortiz, J.B. Foresman, J. Ciolowski, B.B. Stefanov, A. Nanayakkara, M. Challacombe, C.Y. Peng, P.Y. Ayala, W. Chen, M.W. Wong, J.L. Andres, E.S. Replogle, R. Gomberts, R.L Martin, D.J. Fox, J.S. Binkley, D.J. Defrees, J. Baker, J.P. Stewart, M. Head-Gordon, C. Gonzalez, J.A. Pople; Gaussian Inc., Pittsburg PA, 1998.

[25] A.D. Becke, Phys. Rev. A38 (1988) 3098.

[26] J.P. Perdew, Y. Wang, Phys. Rev. B45 (1992) 13244.

[27] P.J. Hay, W.R. Wadt, J. Chem. Phys. 82 (1985) 270.

[28] W.R. Wadt, P.J. Hay, J. Chem. Phys. 82 (1985) 284.

[29] T.H. Dunning, P.J. Hay, in: H.F. SchaeferIII (Ed.), Modern Theoretical Chemistry, Plenum, New York, 1976, pp. 1–28.

[30] T.H. Dunning, Jr., P.J. Hay, Jr., in: H.F. Schaefer, III (Ed.), Modern Theoretical Chemistry, Plenum, New York, 1976, pp. 1–28.

[31] http://www.emsl.pnl.gov:2080/forms/basisform.html